

POSTBUCKLING ANALYSIS OF STIFFENED LAMINATED PANELS LOADED IN COMPRESSION

HUI-SHEN SHEN

Department of Civil Engineering, Shanghai Jiao Tong University, Shanghai 200030,
P.R. China

and

F. W. WILLIAMS

Division of Structural Engineering, University of Wales, College of Cardiff, Cardiff CF2 1XH, U.K.

(Received 29 May 1992; in revised form 2 October 1992)

Abstract—An analytical-numerical method is presented for the postbuckling analysis of prismatic plate structures that may be idealized as an assemblage of laminated, rectangular, plate-strips and beams. The formulations are based on the classical laminated plate theory and include a number of refined features. The analysis uses a deflection-type perturbation technique to determine the buckling loads and the postbuckling equilibrium paths. A computer program has been developed and is used to examine the postbuckling behavior of perfect and imperfect blade stiffened panels, with and without longitudinal, transverse or orthogonal beam stiffeners.

NOTATION

The following is a list of the main symbols used. Other symbols are explained when they are first introduced.

B, B_i	width of entire stiffened panel and plate element ($i = 1, 2, \dots$)
b_1, b_2	width of stiffener
d_1, d_2	distance between centers of stiffeners
E_{11}, E_{22}	elastic moduli for a composite layer
$E_1 A_1, E_2 A_2$	extensional rigidity of stiffeners in the longitudinal and transverse directions
e_1, e_2	stiffener eccentricity
\bar{F}, F	dimensional and nondimensional form of stress function
G_{12}	shear modulus for a composite layer
$G_1 J_1, G_2 J_2$	torsional rigidity of stiffener cross-section
h_1, h_2	height of stiffener
I_1, I_2	moment of inertia of stiffener cross-section about its centroidal axis
L	length of the entire stiffened panel
n_s, n_t	number of stiffeners in the longitudinal and transverse directions
t_i	thickness of rectangular plate element ($i = 1, 2, \dots$)
\bar{W}, W	dimensional and nondimensional form of additional deflection of plate element
\bar{W}^*, W^*	dimensional and nondimensional form of geometrical imperfection of plate element
β	aspect ratio of plate element
ε	a small perturbation parameter
Λ, λ	nondimensional form of load and stress
μ	imperfection parameter
ν_{12}	Poisson's ratio
σ_x, τ_{xy}	average axial stress and shear stress.

INTRODUCTION

Stiffened laminated panels are being used more and more extensively in aerospace structures. These components are expected to achieve their ultimate loads in the postbuckling range. Thus, the initial buckling and postbuckling behavior of stiffened laminated panels must be well understood.

Many studies have been performed for stiffened composite panels under compressive loading. Wittrick and Williams (1972, 1974) developed an accurate buckling analysis for isotropic and anisotropic plate assemblies. Some linear classical buckling loads of stiffened composite panels were obtained analytically by Chiu (1972) and Viswanathan *et al.* (1972, 1973a, b) and experimentally by Spier (1975), Williams and Stein (1976) and Romeo (1986). A design procedure for stiffened composite panels was suggested by Dickson *et al.*

(1980a, b). However, limited progress has been achieved in the methods of postbuckling analysis of stiffened composite panels and only a limited amount of data has been published that describes their postbuckling behavior. Smith (1985), Smith and Dow (1985), Starnes *et al.* (1985) and Wiggenraad (1985) performed experimental studies of postbuckling behavior of stiffened composite panels. Recently, Sheinman *et al.* (1988) and Sheinman and Frostig (1988) developed an analytical-numerical procedure for the buckling and postbuckling behavior of stiffened laminated panels. Moreover, several computer codes (Anderson and Stroud, 1979; Stroud *et al.*, 1984; Dawe and Peshkam, 1989, 1990; Williams *et al.*, 1990; Bushnell, 1987) currently in use have the capability for buckling and postbuckling analysis of stiffened composite panels. These codes are excellent, but in view of the number of degrees of freedom involved are more expensive for parametric study or preliminary design than is the method proposed here.

The present paper is concerned with the buckling and postbuckling of stiffened laminated panels under compressive loading. Attention is confined here to structural components that may, in general, be idealized as an assemblage of laminated plate-strips and beam elements. The individual plate-strip is based on the classical laminated theory and the elementary theory of bending and torsion is used for the beam elements. The initial geometrical imperfections of the plate-strip are taken into account. As many researchers have done, for simplicity the form of initial geometrical imperfection is taken as the buckling mode of relevant plates.

A new approach for postbuckling analysis of isotropic and anisotropic plates has been recently developed by Shen (1989, 1990) and Zhang and Shen (1991), using a deflection-type perturbation technique. Shen and Williams (1993) extended this method to box-type laminated plate assemblies. In contrast, the present study is directed specifically at the postbuckling behavior of stiffened laminated panels. The theory presented is illustrated by some numerical examples of perfect and imperfect blade-stiffened panels. Hence, the analysis and the associated computer program are correlated with existing analytical and test results.

ANALYTICAL FORMULATION

Some of the basic equations from Shen and Williams (1993) are repeated here for clarity, with the very minor changes included that are needed to make them applicable to stiffened panels instead of boxes.

A thin stiffened laminated panel composed of a system of flat plates joined together along their longitudinal edges, with and without interlinked beam stiffeners, is considered. A cross-section is shown in Fig. 1. It is of length L and is loaded in compression. In accordance with most previous theories, the beam stiffeners are averaged or "smeared out" over the stiffener spacing, so that $L = (n_t + 1)d_2$, where n_t is the number of transverse stiffeners. The n_s longitudinal stiffeners of each main skin have spacing d_1 , eccentricity e_1 , height h_1 and width b_1 . e_2 , h_2 and b_2 are defined analogously to e_1 , h_1 and b_1 but are for the transverse stiffeners. Generally, n_s , n_t , d_1 , d_2 , e_1 , e_2 , b_1 , b_2 , h_1 and h_2 can be different for each longitudinal portion into which the plate stiffeners divide the skin.

As described in Shen and Williams (1993), the postbuckling analysis of such structures should be performed by including the following essential features: couple the in-plane and out-of-plane actions along the plate junctions; include the second-order term of in-plane displacement \bar{V} in the end-shortening relationship of the panel; and consider the shear stress along the plate junctions. As a result, the method presented here is different from the classical approximations.

A typical laminated plate-strip forming the plate structures is shown in Fig. 2. \bar{U} , \bar{V} and \bar{W} are the displacements parallel to a right-hand set of axes (x, y, z) as shown. The present analysis for each plate-strip is based on the classical laminated theory, and the elementary theory of bending and torsion is used for the beam stiffeners. Denoting the initial deflection by \bar{W}^* , let \bar{W} be the additional deflection and let the stress function \bar{F} be such that

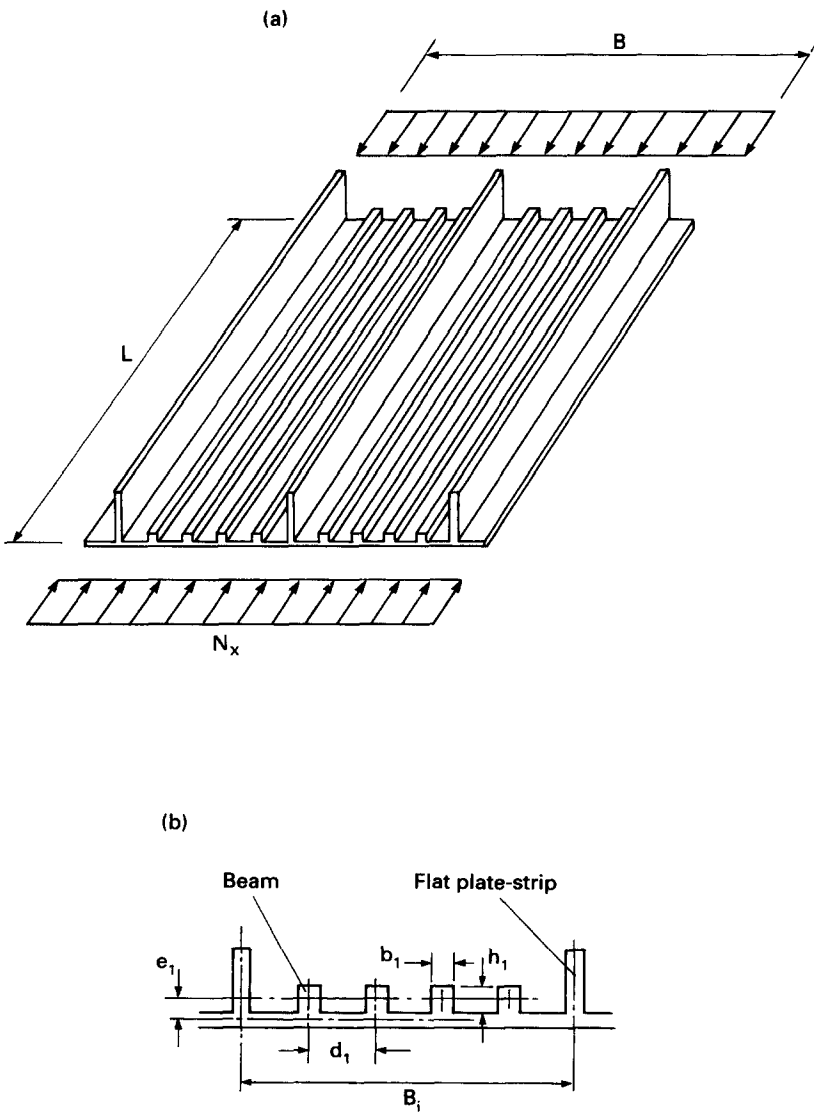


Fig. 1. A typical stiffened laminated panel, showing longitudinal beam stiffeners, but with the transverse stiffeners omitted for clarity.

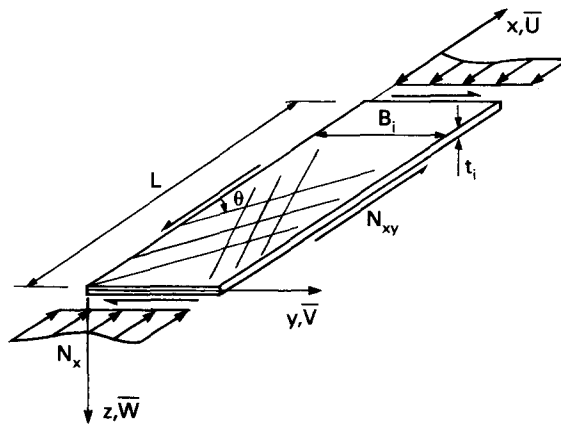


Fig. 2. Laminated plate-strip configuration.

$$N_x = \bar{F}_{,yy}, \quad N_y = \bar{F}_{,xx}, \quad N_{xy} = -\bar{F}_{,xy},$$

then the nonlinear large deflection equations of laminated plates with longitudinal and/or transverse beam-type stiffeners are given as follows:

$$L_1(\bar{W}) + L_3(\bar{F}) = L(\bar{W} + \bar{W}^*, \bar{F}), \quad (1)$$

$$L_2(\bar{F}) - L_3(\bar{W}) = -\frac{1}{2}L(\bar{W} + 2\bar{W}^*, \bar{W}), \quad (2)$$

where

$$\begin{aligned} L_1 &= D_{11}^* \frac{\partial^4}{\partial x^4} + 4D_{16}^* \frac{\partial^4}{\partial x^3 \partial y} + 2(D_{12}^* + 2D_{66}^*) \frac{\partial^4}{\partial x^2 \partial y^2} + 4D_{26}^* \frac{\partial^4}{\partial x \partial y^3} + D_{22}^* \frac{\partial^4}{\partial y^4}, \\ L_2 &= A_{22}^* \frac{\partial^4}{\partial x^4} - 2A_{26}^* \frac{\partial^4}{\partial x^3 \partial y} + (2A_{12}^* + A_{66}^*) \frac{\partial^4}{\partial x^2 \partial y^2} - 2A_{16}^* \frac{\partial^4}{\partial x \partial y^3} + A_{11}^* \frac{\partial^4}{\partial y^4}, \\ L_3 &= B_{21}^* \frac{\partial^4}{\partial x^4} + (2B_{26}^* - B_{61}^*) \frac{\partial^4}{\partial x^3 \partial y} + (B_{11}^* + B_{22}^* - 2B_{66}^*) \frac{\partial^4}{\partial x^2 \partial y^2} \\ &\quad + (2B_{16}^* - B_{62}^*) \frac{\partial^4}{\partial x \partial y^3} + B_{12}^* \frac{\partial^4}{\partial y^4}, \\ L &= \frac{\partial^2}{\partial x^2} \frac{\partial^2}{\partial y^2} - 2 \frac{\partial^2}{\partial x \partial y} \frac{\partial^2}{\partial x \partial y} + \frac{\partial^2}{\partial y^2} \frac{\partial^2}{\partial x^2}, \end{aligned}$$

in these equations, the membrane, coupling and flexural rigidities, including beam stiffener stretching, bending and torsional stiffness, are included. $[A_{ij}^*]$, $[B_{ij}^*]$ and $[D_{ij}^*]$ ($i, j = 1, 2, 6$) are reduced stiffness matrices, defined as

$$\mathbf{A}^* = \mathbf{A}^{-1}, \quad \mathbf{B}^* = -\mathbf{A}^{-1}\mathbf{B}, \quad \mathbf{D}^* = \mathbf{D} - \mathbf{B}\mathbf{A}^{-1}\mathbf{B}$$

and

$$\begin{aligned} \mathbf{A} &= [A_{ij}] + \begin{bmatrix} E_1 A_1 / d_1 & 0 & 0 \\ 0 & E_2 A_2 / d_2 & 0 \\ 0 & 0 & 0 \end{bmatrix}, \\ \mathbf{B} &= [B_{ij}] + \begin{bmatrix} E_1 A_1 e_1 / d_1 & 0 & 0 \\ 0 & E_2 A_2 e_2 / d_2 & 0 \\ 0 & 0 & 0 \end{bmatrix}, \\ \mathbf{D} &= [D_{ij}] + \begin{bmatrix} E_1 (I_1 + A_1 e_1^2) / d_1 & 0 & 0 \\ 0 & E_2 (I_2 + A_2 e_2^2) / d_2 & 0 \\ 0 & 0 & (G_1 J_1 / d_1 + G_2 J_2 / d_2) / 4 \end{bmatrix}, \end{aligned}$$

where $E_1 A_1$, $E_2 A_2$, $G_1 J_1$ and $G_2 J_2$ are the extensional and torsional rigidities of the beam stiffeners in the longitudinal and transverse directions; I_1 and I_2 are the moments of inertia of the beam stiffener cross-sections about their centroidal axes; e_1 and e_2 refer to beam stiffener eccentricities; and details of matrices $[A_{ij}]$, $[B_{ij}]$ and $[D_{ij}]$ ($i, j = 1, 2, 6$) can be found in Chia (1980) and other textbooks.

It is apparent from the expressions for \mathbf{A} , \mathbf{B} and \mathbf{D} given above that stiffeners are assumed to stiffen the panel only in the directions of their lengths, so that it is implied that the values of b_1/d_1 and b_2/d_2 are not excessive. This implied approximation is shared by most previous "smeared stiffener" papers and so is not discussed further here.

The unit end-shortening relationship is

$$\begin{aligned} \frac{\Delta_x}{L} &= -\frac{1}{LB_i} \int_0^{B_i} \int_0^L \frac{\partial \bar{U}}{\partial x} dx dy \\ &= -\frac{1}{LB_i} \int_0^{B_i} \int_0^L \left\{ \left[A_{11}^* \frac{\partial^2 \bar{F}}{\partial y^2} + A_{12}^* \frac{\partial^2 \bar{F}}{\partial x^2} - A_{16}^* \frac{\partial^2 \bar{F}}{\partial x \partial y} \right] - \left[B_{11}^* \frac{\partial^2 \bar{W}}{\partial x^2} \right. \right. \\ &\quad \left. \left. + B_{12}^* \frac{\partial^2 \bar{W}}{\partial y^2} + 2B_{16}^* \frac{\partial^2 \bar{W}}{\partial x \partial y} \right] - \frac{1}{2} \left[\left(\frac{\partial \bar{U}}{\partial x} \right)^2 + \left(\frac{\partial \bar{V}}{\partial x} \right)^2 + \left(\frac{\partial \bar{W}}{\partial x} \right)^2 \right] - \frac{\partial \bar{W}}{\partial x} \frac{\partial \bar{W}^*}{\partial x} \right\} dx dy. \end{aligned} \quad (3)$$

The corresponding boundary conditions are

$$x = 0, L, \quad \bar{W} = \bar{V} = 0, \quad (4a)$$

$$\int_0^{B_i} N_x dy + \sigma_x t_i B_i = 0, \quad (4b)$$

$$\int_0^{B_i} N_{xy} dy - \tau_{xy} t_i B_i = 0. \quad (4c)$$

Introducing nondimensional quantities and omitting the subscript *i* when convenient :

$$\begin{aligned} x &= \pi x/L, \quad y = \pi y/B_i, \quad \beta = L/B_i, \quad (W^*, W, U, V) = (\bar{W}^*, \bar{W}, \bar{U}, \bar{V}) / \sqrt{D_{11}^* D_{22}^* A_{11}^* A_{22}^*}, \\ F &= \bar{F} / \sqrt{D_{11}^* D_{22}^*}, \quad \gamma_5 = -A_{12}^* / A_{22}^*, \quad \gamma_6 = L / \pi \sqrt{D_{11}^* D_{22}^* A_{11}^* A_{22}^*}, \\ (\gamma_{11}, \gamma_{12}, \gamma_{13}) &= (D_{16}^*, D_{12}^* + 2D_{66}^*, D_{26}^*) / D_{11}^*, \quad \gamma_{14} = \sqrt{D_{22}^* / D_{11}^*}, \\ (\gamma_{21}, \gamma_{22}, \gamma_{23}) &= (A_{26}^*, A_{12}^* + A_{66}^* / 2, A_{16}^*) / A_{22}^*, \quad \gamma_{24} = \sqrt{A_{11}^* / A_{22}^*}, \\ (\gamma_{30}, \gamma_{31}, \gamma_{32}, \gamma_{33}, \gamma_{34}, \gamma_{311}, \gamma_{316}) & \\ &= (B_{21}^*, 2B_{26}^* - B_{61}^*, B_{11}^* + B_{22}^* - 2B_{66}^*, 2B_{16}^* - B_{62}^*, B_{12}^*, B_{11}^*, B_{16}^*) / \sqrt{D_{11}^* D_{22}^* A_{11}^* A_{22}^*}, \\ (\lambda_x, \lambda_{xy}) &= (\sigma_x, \tau_{xy}) t_i B_i^2 / 4\pi^2 \sqrt{D_{11}^* D_{22}^*}, \\ \delta_x &= (\Delta_x / L) B_i^2 / 4\pi^2 \sqrt{D_{11}^* D_{22}^* A_{11}^* A_{22}^*} \end{aligned}$$

enables the nonlinear equations (1) and (2) to be written in the nondimensional form

$$L_1(W) + \gamma_{14} L_3(F) = \gamma_{14} \beta^2 L(W + W^*, F), \quad (5)$$

$$L_2(F) - \gamma_{24} L_3(W) = -\frac{1}{2} \gamma_{24} \beta^2 L(W + 2W^*, W), \quad (6)$$

where

$$\begin{aligned} L_1 &= \frac{\partial^4}{\partial x^4} + 4\gamma_{11} \beta \frac{\partial^4}{\partial x^3 \partial y} + 2\gamma_{12} \beta^2 \frac{\partial^4}{\partial x^2 \partial y^2} + 4\gamma_{13} \beta^3 \frac{\partial^4}{\partial x \partial y^3} + \gamma_{14}^2 \beta^4 \frac{\partial^4}{\partial y^4}, \\ L_2 &= \frac{\partial^4}{\partial x^4} - 2\gamma_{21} \beta \frac{\partial^4}{\partial x^3 \partial y} + 2\gamma_{22} \beta^2 \frac{\partial^4}{\partial x^2 \partial y^2} - 2\gamma_{23} \beta^3 \frac{\partial^4}{\partial x \partial y^3} + \gamma_{24}^2 \beta^4 \frac{\partial^4}{\partial y^4}, \\ L_3 &= \gamma_{30} \frac{\partial^4}{\partial x^4} + \gamma_{31} \beta \frac{\partial^4}{\partial x^3 \partial y} + \gamma_{32} \beta^2 \frac{\partial^4}{\partial x^2 \partial y^2} + \gamma_{33} \beta^3 \frac{\partial^4}{\partial x \partial y^3} + \gamma_{34} \beta^4 \frac{\partial^4}{\partial y^4}, \\ L &= \frac{\partial^2}{\partial x^2} \frac{\partial^2}{\partial y^2} - 2 \frac{\partial^2}{\partial x \partial y} \frac{\partial^2}{\partial x \partial y} + \frac{\partial^2}{\partial y^2} \frac{\partial^2}{\partial x^2}. \end{aligned}$$

The unit end-shortening relationship becomes

$$\delta_x = -\frac{1}{4\pi^2\beta^2\gamma_{24}} \int_0^\pi \int_0^\pi \left\{ \left[\gamma_{24}^2\beta^2 \frac{\partial^2 F}{\partial y^2} - \gamma_5 \frac{\partial^2 F}{\partial x^2} - \gamma_{23}\beta \frac{\partial^2 F}{\partial x \partial y} \right] - \gamma_{24} \left[\gamma_{311} \frac{\partial^2 W}{\partial x^2} + \gamma_{34}\beta^2 \frac{\partial^2 W}{\partial y^2} + 2\gamma_{316}\beta \frac{\partial^2 W}{\partial x \partial y} \right] - \frac{1}{2}\gamma_{24} \left[\left(\frac{\partial U}{\partial x} \right)^2 + \left(\frac{\partial V}{\partial x} \right)^2 + \left(\frac{\partial W}{\partial x} \right)^2 \right] - \gamma_{24} \frac{\partial W}{\partial x} \frac{\partial W^*}{\partial x} \right\} dx dy \quad (7)$$

and the boundary conditions become

$$x = 0, \pi, \quad W = V = 0, \quad (8a)$$

$$\frac{1}{\pi} \int_0^\pi \beta^2 \frac{\partial^2 F}{\partial y^2} dy + 4\lambda_x \beta^2 = 0, \quad (8b)$$

$$\frac{1}{\pi} \int_0^\pi \beta^2 \frac{\partial^2 F}{\partial x \partial y} dy + 4\lambda_{xy} \beta^2 = 0. \quad (8c)$$

Applying eqns (5)–(8), the postbuckling behavior of each plate-strip under combined axial compression and shear force can be determined by the perturbation technique suggested in Shen (1989, 1990) and Zhang and Shen (1991).

To construct an asymptotic solution for the laminated plate, the additional deflection and stress functions in eqns (5) and (6) are both taken in the form of perturbation expansions as

$$W(x, y, \varepsilon) = \sum_{j=1} \varepsilon^j w_j(x, y), \quad F(x, y, \varepsilon) = \sum_{j=0} \varepsilon^j f_j(x, y) \quad (9)$$

and the first term of $w_j(x, y)$ is assumed to have the form

$$w_1(x, y) = A_{11}^{(1)} \sin mx \sin n(y+kx).$$

The initial imperfection is assumed to have a similar form :

$$W^*(x, y, \varepsilon) = \varepsilon A_{11}^* \sin mx \sin n(y+kx) = \varepsilon \mu A_{11}^{(1)} \sin mx \sin n(y+kx), \quad (10)$$

in which the imperfection parameter $\mu = A_{11}^*/A_{11}^{(1)}$.

Substituting eqns (9) and (10) into eqns (5) and (6), by using a perturbation procedure, the amplitudes in terms of $w_j(x, y)$ and $f_j(x, y)$ can be determined step by step, and the asymptotic solutions are obtained as follows :

$$\begin{aligned} W = & \varepsilon [A_{11}^{(1)} \sin mx \sin n(y+kx)] + \varepsilon^2 [A_{20}^{(2)} \cos 2mx + A_{02}^{(2)} \cos 2n(y+kx)] \\ & + \varepsilon^3 [A_{13}^{(3)} \sin mx \sin 3n(y+kx) + A_{31}^{(3)} \sin 3mx \sin n(y+kx)] \\ & + D_{13}^{(3)} \cos mx \cos 3n(y+kx) + D_{31}^{(3)} \cos 3mx \cos n(y+kx)] + O(\varepsilon^4), \quad (11) \end{aligned}$$

$$\begin{aligned}
 F = & -B_{00}^{(0)} \frac{y^2}{2} - C_{00}^{(0)} xy + \varepsilon [B_{11}^{(1)} \sin mx \sin n(y+kx) \\
 & + C_{11}^{(1)} \cos mx \cos n(y+kx)] + \varepsilon^2 \left[-B_{00}^{(2)} \frac{y^2}{2} - C_{00}^{(2)} xy + B_{20}^{(2)} \cos 2mx \right. \\
 & \left. + B_{02}^{(2)} \cos 2n(y+kx) \right] + \varepsilon^3 [B_{11}^{(3)} \sin mx \sin n(y+kx) \\
 & + B_{13}^{(3)} \sin mx \sin 3n(y+kx) + B_{31}^{(3)} \sin 3mx \sin n(y+kx) \\
 & + C_{11}^{(3)} \cos mx \cos n(y+kx) + C_{13}^{(3)} \cos mx \cos 3n(y+kx) \\
 & + C_{31}^{(3)} \cos 3mx \cos n(y+kx)] + O(\varepsilon^4). \tag{12}
 \end{aligned}$$

As pointed out in Shen and Williams (1993), the solution of eqn (11) does not satisfy the boundary condition of eqn (8a) exactly, because prebuckling deformations are ignored.

Note that in eqns (11) and (12), the coefficients are related and can all be written as functions of $A_{11}^{(1)}$ [see Appendix II in Shen and Williams (1993)].

Substituting eqn (12) into boundary conditions (8b) and (8c) gives [where $\lambda_x^{(0)}, \lambda_x^{(2)}; \lambda_{xy}^{(0)}, \lambda_{xy}^{(2)}; \Theta_1, \Theta_2$; and $\delta_x^{(0)}, \delta_x^{(2)}$ are given in detail in Shen and Williams (1993)]

$$\lambda_x = \lambda_x^{(0)} + \lambda_x^{(2)} (A_{11}^{(1)} \varepsilon)^2 + \dots, \tag{13}$$

$$\lambda_{xy} = \lambda_{xy}^{(0)} + \lambda_{xy}^{(2)} (A_{11}^{(1)} \varepsilon)^2 + \dots, \tag{14}$$

in which $(A_{11}^{(1)} \varepsilon)$ can be written as a function of the deflection of the plate. If the maximum deflection is taken at the point $(x, y) = (\pi/2m, \pi/2n - k\pi/2m)$, then

$$A_{11}^{(1)} \varepsilon = W_m + (\Theta_1 + \Theta_2) W_m^2 + \dots \tag{15}$$

Using eqn (7), together with eqns (11) and (12), we have

$$\delta_x = \delta_x^{(0)} + \delta_x^{(2)} (A_{11}^{(1)} \varepsilon)^2 + \dots \tag{16}$$

Thus, treating k and $(A_{11}^{(1)} \varepsilon)$ as two unknown variables, there are three equations, (13), (14) and (16), from which it is possible to determine the axial stress, shear stress and end-shortening for each plate-strip.

Further, for postbuckling analysis of the entire panel, the compatibility conditions require that

$$\sum_{j=1} (\tau_{xy})_j = 0 \quad (\text{at common junction}), \tag{17}$$

$$(\Delta_x/L)_i = (\Delta_x/L)_{i+1}, \tag{18}$$

and the half-wave numbers in the longitudinal direction of all buckled plates are the same. From the above conditions, together with the boundary conditions of longitudinal edges, which are simply supported ($\bar{U} = \bar{W} = 0$) or free, the other unknown variables k_i and $(A_{11}^{(1)} \varepsilon)_i$ ($i = 2, 3, \dots$) can be determined.

Rewriting eqn (13), the postbuckling equilibrium path of the stiffened panel can be written as

$$\Lambda = \sum_{i=1} [\Lambda_i^{(0)} + \Lambda_i^{(2)} (A_{11}^{(1)} \varepsilon)_i^2 + \dots]. \tag{19}$$

This equation characterizes the postbuckling load-deflection curves of stiffened laminated panels loaded in compression. The buckling load of perfect panels can also readily be obtained numerically, by setting $\mu = 0$ (or $\bar{W}^*/t = 0$), while taking $W_m = 0$ (or $\bar{W}/t = 0$).

NUMERICAL EXAMPLES AND DISCUSSION

The buckling and postbuckling behavior of a stiffened laminated panel was investigated analytically using a program developed for the purpose and many examples have been solved numerically. Here attention is confined to blade stiffened laminated panels.

First, consideration is given to the initial buckling of a blade stiffened composite panel and the results are compared with results in the literature. The overall geometry of the blade stiffened panel and the stiffener and skin layup details are shown in Fig. 3. The panel was considered as the third example of seven in a NASA report by Stroud *et al.* (1984). All plies of the main skin and the stiffeners are graphite-epoxy with properties given as: $E_{11} = 131.0$ GPa; $E_{22} = 13.0$ GPa; $G_{12} = 6.41$ GPa; and $\nu_{12} = 0.38$. Stroud *et al.* (1984) quote their buckling results in terms of a load factor which is the factor by which the prescribed prebuckling applied loads per unit width of panel, $= 175.13$ N mm⁻¹, are multiplied to cause initial buckling. The same load factor, designated f , is adopted here when presenting and comparing the results obtained by using VIPASA (Wittrick and Williams, 1974), BAVAMPAC (Peshkam and Dawe, 1988), EAL (Stroud *et al.*, 1984) and FEM (Tripathy and Rao, 1992), which are given in Table 1.

The second example deals with a blade stiffened carbon-epoxy panel with symmetrical stiffeners and symmetrical (S) and nonsymmetrical (NS) skins. The cross-section and the stiffener and skin layup details are shown in Fig. 4. The length of panel is, in turn, either $L = 1100$ mm or $L = 340$ mm. The layer material properties are: $E_{11} = 115.0$ GPa; $E_{22} = 7.1$ GPa; $G_{12} = 4.0$ GPa; $\nu_{12} = 0.31$; and thickness $t_{ply} = 0.2$ mm. The buckling load and the end-shortening calculated are listed in Table 2, where they are compared with test and analytical results given by Wiggeraad (1985). Clearly, the results obtained from the present method accord quite well with the test results.

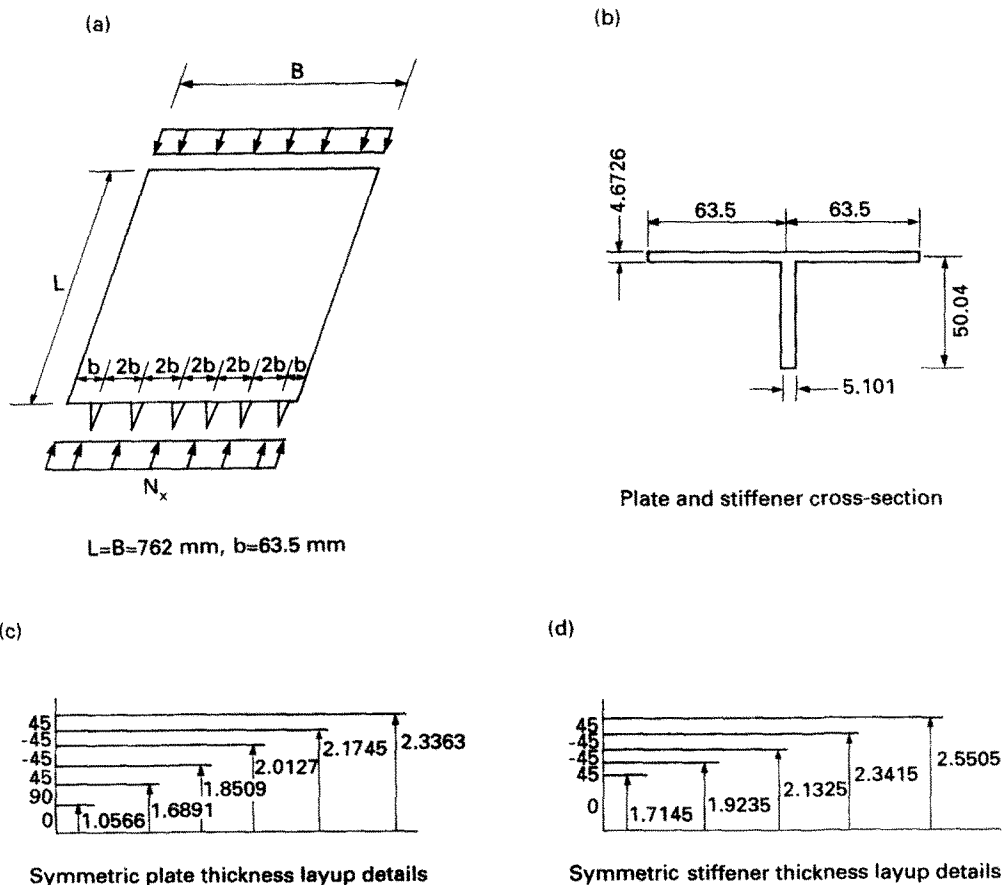


Fig. 3. Geometry and loading of a blade stiffened panel (Example 1).

Table 1. Initial buckling of blade stiffened graphite-epoxy panel : values of load factor f

Boundary conditions (longitudinal edges)	VIPASA†	BAVAMPAC‡	EAL§	FEM	Present
$\bar{U} = \bar{W} = 0$	9.97	9.97	10.076	11.81	10.64
free	9.24				9.49

†VIPASA (Wittrick and Williams, 1974).

‡BAVAMPAC (Peshkam and Dawe, 1989).

§EAL (Stroud *et al.*, 1984).

|| FEM (Tripathy and Rao, 1992).

stiffener type a: $[\pm 0_6/\mp 45]_T$

symmetrical skin (S): $[\mp 45/0_3/\pm 45]_T$

stiffener type b: $[\mp 45/0_6/\pm 45]_T$

non-symmetrical skin (NS): $[\pm 45/0_3/\pm 45]_T$

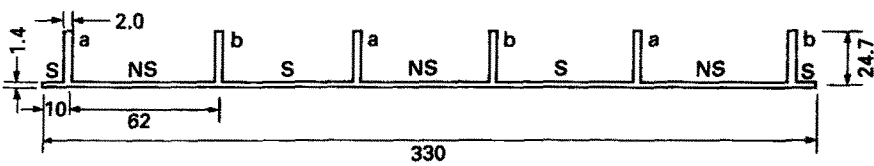


Fig. 4. Geometry of a blade stiffened panel (Example 2).

The third example concerns a graphite-epoxy open section stiffened by a blade type. The data used here are from Sheinman and Frostig (1988), as shown in Fig. 5. The length of panel is taken to be $L = 187.5$ mm and material properties are: $E_{11} = 131.0$ GPa; $E_{22} = 13.0$ GPa; $G_{12} = 6.41$ GPa; and $\nu_{12} = 0.38$. The initial imperfection (for the skin

Table 2. Comparisons of initial buckling load and end-shortening of blade stiffened carbon-epoxy panels

L (mm)		Wiggenraad (1985)		
		Experimental	Analytical	Present
1100	Buckling load (kN)	87	89	87.63
	End-shortening (mm)	1.86	1.86	1.96
340	Buckling load (kN)	100	102	100.08
	End-shortening (mm)	0.70	0.64	0.69

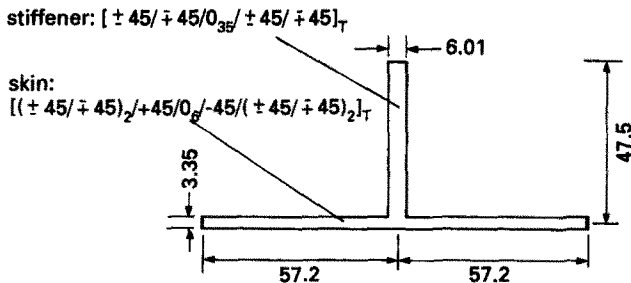


Fig. 5. Geometry of a blade stiffened panel (Example 3).

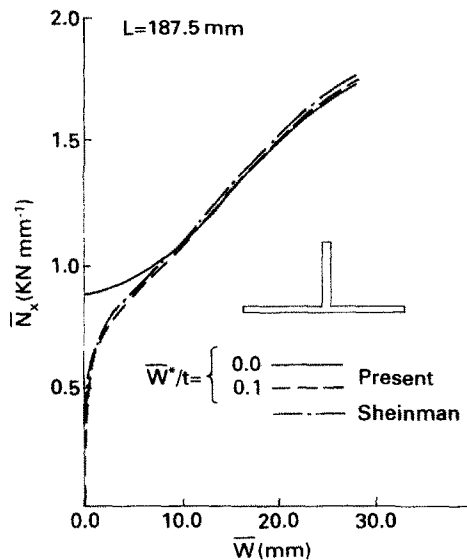


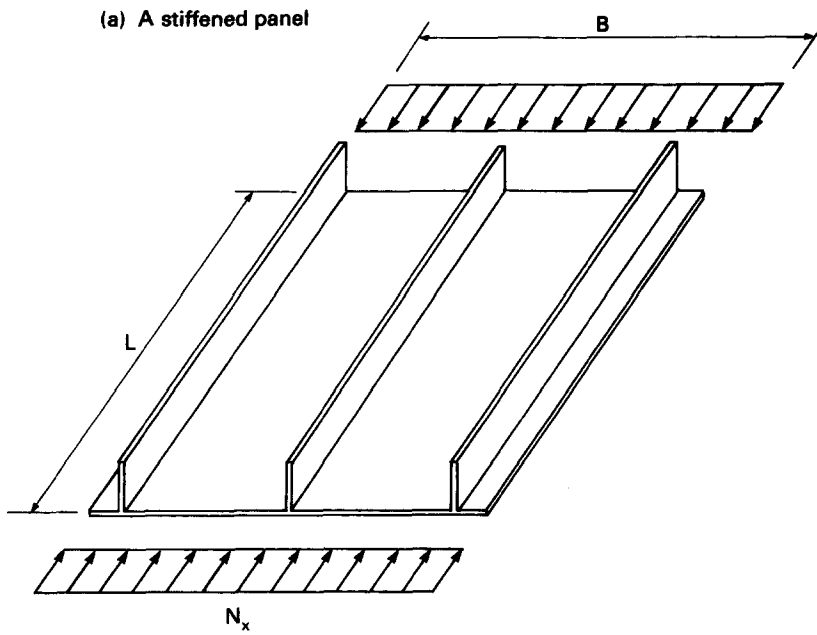
Fig. 6. Load-deflection curves of stiffened panel (Example 3).

only) is taken to be $\bar{W}^* = 0.335$ mm, so that $\bar{W}^*/t = 0.1$. The authors' analytical post-buckling load-deflection curves are shown in Fig. 6 to compare well with that given by Sheinman and Frostig (1988), when the initial skin imperfection is taken into account.

The good correlation between the authors' results and the other results of Tables 1 and 2 and Fig. 6 demonstrates the acceptable accuracy of the method presented.

Next, blade stiffened graphite-epoxy laminated panels with and without longitudinal, transverse or orthogonal beam stiffeners are considered. The overall geometry of the stiffened panel, the loading, the stiffener and skin layup details are shown in Fig. 7. The length of the panel is taken to be $L = 644.0$ mm and material properties are: $E_{11} = 131.0$ GPa; $E_{22} = 13.0$ GPa; $G_{12} = 6.41$ GPa; and $\nu_{12} = 0.38$. For convenience, when beam stiffeners were added they had: the number of longitudinal beam stiffeners for each of the two main skin portions (of width 140 mm in Fig. 7) was $n_s = 4$; the number of transverse beam stiffeners of each skin portion was $n_t = 22$; the widths of the beam stiffeners were $b_1 = b_2 = 7.62$ mm; the heights of the beam stiffeners were $h_1 = h_2 = 12.7$ mm; and the beam stiffener material properties were $E_1 = E_2 = 72.4$ GPa and $G_1 = G_2 = 27.4$ GPa.

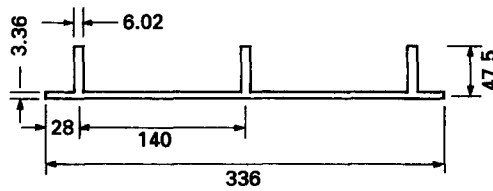
Analytical postbuckling load-deflection curves for the perfect and imperfect blade stiffened panel without the beam stiffeners are plotted in Fig. 8(a). Results with longitudinal beam stiffeners are plotted in Fig. 8(b), results with transverse beam stiffeners are plotted in Fig. 8(c) and results with orthogonal beam stiffeners are plotted in Fig. 8(d). It can be seen that the stiffened panel with orthogonal beam stiffeners has the highest initial buckling load and the highest postbuckling load. However, the curves for the perfect panels of Fig. 8 show that, for any permitted postbuckled deflection \bar{W}/t , the percentage by which the postbuckling load exceeds the initial buckling load is much higher for the panel with longitudinal beam stiffeners than for the panels with no beam stiffeners or with orthogonal beam stiffeners, and is virtually nonexistent for the panel with transverse beam stiffeners. This pattern of postbuckling behavior is largely mirrored by the imperfect results. Thus the postbuckling behavior is by far the most favorable for the panel with longitudinal beam stiffeners and has significant benefits for the panels with no beam stiffeners or with orthogonal ones. However, it is unfavorable for the panel with transverse stiffeners, such that the maximum load achieved is about 87% of the initial buckling load at about $\bar{W} = t$ and decreases slightly as \bar{W} increases beyond this, so that the panel is sensitive to initial imperfections. Comparison of Figs 8(a) with 8(c), and 8(b) with 8(d), shows that the addition of transverse beam stiffeners always increases the initial buckling and postbuckling loads, but with the percentage increase of the former considerably higher than for the latter, so that the addition of the transverse beams has led to less favorable postbuckling behavior.



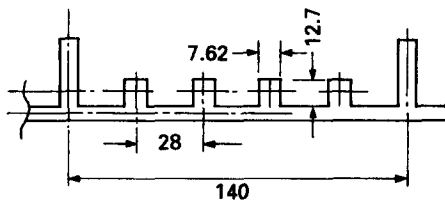
(b) Cross-section (without beam stiffeners)

stiffener: $[\pm 45/\mp 45/0_{35}/\pm 45/\mp 45]_T$

skin: $[(\pm 45/\mp 45)_2/\mp 45/0_g/\mp 45/(\pm 45/\mp 45)_2]_T$



(c) Longitudinal beam stiffeners



(d) Transverse beam stiffeners

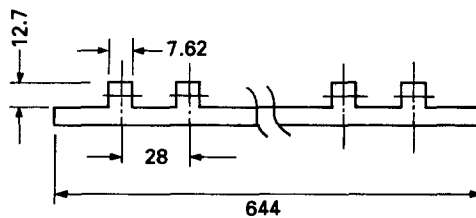


Fig. 7. Geometry and loading of a blade stiffened panel (Example 4).

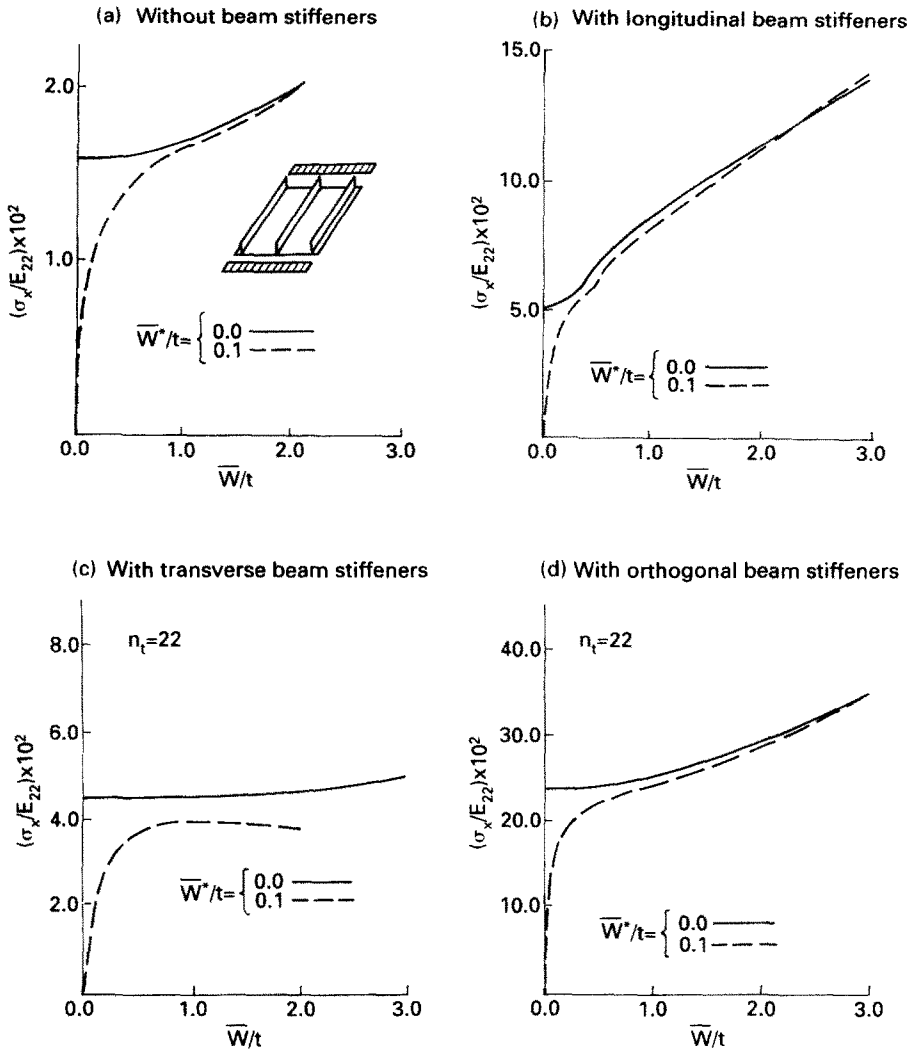


Fig. 8. Load-deflection curves of stiffened panels.

CONCLUSIONS

The postbuckling analysis and an analytical-numerical procedure have been presented for stiffened laminated panels. A number of examples have been given to illustrate their applications, which relate to the performance of perfect and imperfect blade stiffened laminated panels with and without beam stiffeners. Numerical correlation with existing analysis and test data is reasonably good.

The solution methodology is general in nature and suitable for: (1) any type of stiffened panels with and without beam stiffeners, subject to the usual limitations of "smeared stiffener" theory; (2) arbitrary stacking combination and orientation of the laminates in the panel skin and stiffener components; (3) any imperfection geometry and; (4) initial buckling as well as postbuckling analysis.

REFERENCES

- Anderson, M. S. and Stroud, W. J. (1979). A general panel sizing computer code and its application to composite structural panels. *AIAA JI* 17(8), 892-897.
- Bushnell, D. (1987). PANDA2-program for minimum weight design of stiffened, composite, locally buckled panels. *Comput. Struct.* 25(4), 469-605.
- Chia, C. Y. (1980). *Nonlinear Analysis of Plates*. McGraw-Hill, New York.
- Chiu, K. D. (1972). Stability of orthotropic stiffened composite plates. *ASCE J. Engng Mech.* 98(5), 1253-1271.

- Dawe, D. J. and Peshkam, V. (1990). A buckling analysis capability for use in the design of composite prismatic plate structures. *Compos. Struct.* **16**, 33–63.
- Dickson, J. N., Biggers, S. B. and Wang, J. T. S. (1980a). A preliminary design procedure for composite panels with open-section stiffeners loaded in the post-buckling range. In *Advances in Composite Materials* (Edited by A. R. Bunsell, C. Bathias, A. Martrenchar, D. Menkes and G. Verchery), pp. 812–825. Pergamon Press, Oxford.
- Dickson, J. N., Cole, R. T. and Wang, J. T. S. (1980b). Design of stiffened composite panels in the post-buckling range. In *Fibrous Composites in Structural Design* (Edited by E. M. Lenoe, D. W. Oplinger and J. J. Burke), pp. 313–327. Plenum Press, New York.
- Peshkam, V. and Dawe, D. J. (1989). Buckling and vibration of finite-length composite prismatic plate structures with diaphragm ends. Part II: Computer programs and buckling applications. *Comput. Meth. Appl. Mech. Engng* **77**, 227–252.
- Romeo, G. (1986). Experimental investigation on advanced composite-stiffened structures under uniaxial compression and bending. *AIAA JI* **24**(11), 1823–1830.
- Sheinman, I. and Frostig, Y. (1988). Post-buckling analysis of stiffened laminated panel. *ASME J. Appl. Mech.* **55**(3), 635–640.
- Sheinman, I., Frostig, Y. and Segal, A. (1988). Bifurcation buckling analysis of stiffened laminated composite panels. In *Buckling of Structures: Theory and Experiment* (Edited by I. Elishakoff, J. Arbocz, C. D. Babcock and A. Libai), pp. 355–381. Elsevier, Amsterdam.
- Shen, H. (1989). Postbuckling behavior of rectangular plates under combined loading. *Thin-Walled Struct.* **8**(3), 203–216.
- Shen, H. (1990). Buckling and postbuckling behavior of antisymmetrically angle-ply laminated composite plates. *Appl. Math. Mech.* **11**(12), 1155–1165.
- Shen, H. and Williams, F. W. (1993). Postbuckling analysis of stiffened laminated box columns. *ASCE J. Engng Mech.* **119**(1), 39–57.
- Smith, C. S. (1985). Compressive strength of transversely stiffened FRP panels. In *Aspects of the Analysis of Plate Structures* (Edited by D. J. Dawe, R. W. Horsington, A. G. Kamtekar and G. H. Little), pp. 149–174. Oxford University Press, Oxford.
- Smith, C. S. and Dow, R. S. (1985). Compressive strength of longitudinally stiffened GRP panels. In *Composite Structures 3* (Edited by I. H. Marshall), pp. 468–490. Elsevier, Amsterdam.
- Spier, E. E. (1975). Crippling/column buckling analysis and test of graphite/epoxy stiffened panels *Proc. AIAA/ASME/SAE 16th Struct., Struct. Dyn. and Materials Conf.*, Part 1, pp. 1–15.
- Starnes, J. H., Knight, N. F. and Rouse, M. (1985). Postbuckling behavior of selected flat stiffened graphite-epoxy panels loaded in compression. *AIAA JI* **23**(8), 1236–1246.
- Stroud, W. J., Greene, W. H. and Anderson, M. S. (1984). Buckling loads of stiffened panels subjected to combined longitudinal compression and shear: results obtained with PASCO, EAL and STAGS computer programs. NASA TP-2215.
- Tripathy, B. and Rao, K. P. (1992). Stiffened composite cylindrical panels—optimum lay-up for buckling by ranking. *Comput. Struct.* **42**(4), 481–488.
- Viswanathan, A. V., Soong, T. C. and Miller, R. E. (1972). Buckling analysis for structural sections and stiffened plates reinforced with laminated composites. *Int. J. Solids Structures* **8**(3), 347–367.
- Viswanathan, A. V., Soong, T. C. and Miller, R. E. (1973a). Compressive buckling analysis and design of stiffened flat plates with multilayered composite reinforcement. *Comput. Struct.* **3**(2), 281–297.
- Viswanathan, A. V., Tamekuni, M. and Tripp, L. L. (1973b). Elastic stability of biaxially loaded longitudinally stiffened composite structures. *AIAA JI* **11**(11), 1553–1559.
- Wiggenraad, J. F. M. (1985). The postbuckling behavior of blade stiffened carbon/epoxy panels loaded in compression. NLR (National Lucht en Ruimteruimtelaboratorium) MP-85019U, The Netherlands.
- Williams, F. W. and Wittrick, W. H. (1972). Numerical results for the initial buckling of some stiffened panels in compression. *Aero. Q.* **23**, 24–40.
- Williams, F. W., Kennedy, D. and Anderson, M. S. (1990). Analysis features of VICONOPT, an exact buckling and vibration program for prismatic assemblies of anisotropic plates. *Proc. 31st AIAA/ASME/ASCE/AHS/ASC Struct., Struct. Dyn. and Materials Conf.*, Part 2, pp. 920–929.
- Williams, J. G. and Stein, M. (1976). Buckling behavior and structural efficiency of open-section stiffened composite compression panels. *AIAA JI* **14**(11), 1618–1626.
- Wittrick, W. H. and Williams, F. W. (1974). Buckling and vibration of anisotropic or isotropic plate assemblies under combined loadings. *Int. J. Mech. Sci.* **16**, 209–239.
- Zhang, J. W. and Shen, H. S. (1991). Postbuckling of orthotropic rectangular plates in biaxial compression. *ASCE J. Engng Mech.* **117**(5), 1158–1170.